

## NOTE

## An algorithm for stereotactic localization by computed tomography or magnetic resonance imaging

Jianrong Dai<sup>1</sup>, Yunping Zhu<sup>1</sup>, Huamin Qu<sup>2</sup> and Yimin Hu<sup>3</sup>

<sup>1</sup> Department of Radiation Oncology, St Jude Children's Research Hospital, Memphis, TN 38105, USA

<sup>2</sup> Center for Visual Computing and Department of Computer Science, State University of New York at Stony Brook, Stony Brook, NY 11794, USA

<sup>3</sup> Department of Radiation Oncology, Cancer Hospital (Institute), Chinese Academy of Medical Sciences, Beijing 100021, People's Republic of China

E-mail: jianrong.dai@stjude.org

Received 13 June 2000

### Abstract

Stereotactic localization of an intracranial lesion by computed tomography or magnetic resonance imaging requires the use of a head frame that is fixed to the skull of the patient. To such head frames are attached either N-shaped or V-shaped localization rods. Because of patient positioning, the transverse imaging slices may not be parallel to the frame base; a coordinate transformation algorithm that takes this possibility into consideration is crucial. Here we propose such an algorithm for a head frame with V-shaped localization rods. Our algorithm determines the transformation matrix between the image coordinate system of a transverse image and the frame coordinate system. The determining procedure has three steps: (a) calculation of the oblique angles of a transverse image relative to the head frame and calculation of the image magnification factor; (b) determination of the coordinates of four central markers in both coordinate systems; and (c) determination of the  $3 \times 3$  transformation matrix by using the coordinates of the four markers. This algorithm is robust in principle and is useful for improving the accuracy of localization.

### 1. Introduction

The purpose of stereotactic radiosurgery or radiotherapy is to deliver a highly focused dose of radiation to a target volume while sparing surrounding normal tissues. Achieving this purpose requires accurate localization of the target volume and accurate alignment of the prescribed dose distribution to the localized target volume (Serago *et al* 1991, Hartmann *et al* 1994, Yeung *et al* 1994). For a patient with an intracranial lesion, these requirements are usually satisfied by using a head localization frame (Leksell 1983, Hartmann *et al* 1985, Lutz *et al* 1988). Working as a coordinate system, the localization frame is fixed to the skull of the patient during

computed tomography (CT) or magnetic resonance (MR) imaging or angiography. For CT or MR imaging, N-shaped (e.g. Radionics, Burlington, USA) or V-shaped (e.g. Fischer, Freiburg, Germany) localization rods are attached to the frame, whereas for angiography, small radio-opaque balls are attached. These localization rods and radio-opaque balls create markers on the images. Once the positions of the markers on an image have been detected, a coordinate transformation matrix between the image coordinate system (ICS) and the frame coordinate system (FCS) can be determined. The use of this matrix allows determination of the coordinates of the target and of other critical organs in the FCS from their coordinates in the ICS. Without mechanical adjustment, the coordinate transformation includes three freedoms of rotation and three freedoms of translation. Through repeatedly adjusting the position of the localization frame, the three freedoms of rotation can be eliminated and the transformation is simplified to include only three freedoms of translation. However, the adjustment is labour intensive. A more desirable method is to develop robust algorithms that can deal with both rotations and translations. Three such algorithms have been proposed for a frame with N-shaped localization rods (Brown *et al* 1980, Saw *et al* 1987, Grunert and Maurer 1995), and one such algorithm has been proposed for target localization with biplanar angiographic imaging (Siddon and Barth 1987). Here we propose a corresponding robust algorithm for a frame with V-shaped localization rods. To our knowledge, this algorithm is the first to be developed for the V-shaped frame.

## 2. Methods

### 2.1. CT or MR imaging

Our algorithm is based on the geometry of the head frame of Fischer. The head frame has four localization planes, each of which contains three localization rods that form a 'V' shape (figure 1(a)). The half angle of 'V' is  $\arctan(0.5)$  (e.g.  $26.565^\circ$ ). The base of the frame is a square. The FCS is set up as follows: the origin is at the centre of the frame base; the  $X$ -axis points to the right side of the patient's head, the  $Y$ -axis points toward the front of the patient, and both axes are on the plane of the frame base; and the  $Z$ -axis points in the supracranial direction. In the following description, a point is represented by a capital letter in the FCS and a lower case letter in the ICS; a line section is represented by two capital letters in the FCS and two lower case letters in the ICS; and the half angle of 'V' is represented by a symbol ' $v$ ' (e.g.  $v = 26.565^\circ$ ). The coordinates of points and the lengths of line sections are in millimetres in the FCS and in image pixels in the ICS.

If transverse CT or MR images are parallel to the frame base, we observe the following four characteristics (figure 1(b)):

- (a) Symmetrical distribution of 12 markers. Lines drawn through three markers of each localization plane result in a square.
- (b) Equal distance between the  $i$ th and the  $j$ th markers when  $i$  is equal to 1, 2, 4, 5, 7, 8, 10 or 11, and  $j$  is equal to  $i + 1$ .
- (c) Equal  $Z$  coordinates in the FCS. The  $Z$  coordinate of an arbitrary point is equal to the distances between the  $i$ th and the  $j$ th markers when  $i$  is equal to 1, 4, 7 or 10, and  $j$  is equal to  $i + 2$ .
- (d) Translation, but no rotation, in the coordinate transformation between the ICS and the FCS.

In this case, the procedure to determine the coordinate transformation between the ICS and the FCS is so simple that no references exist to support it. To be clear, here we use the

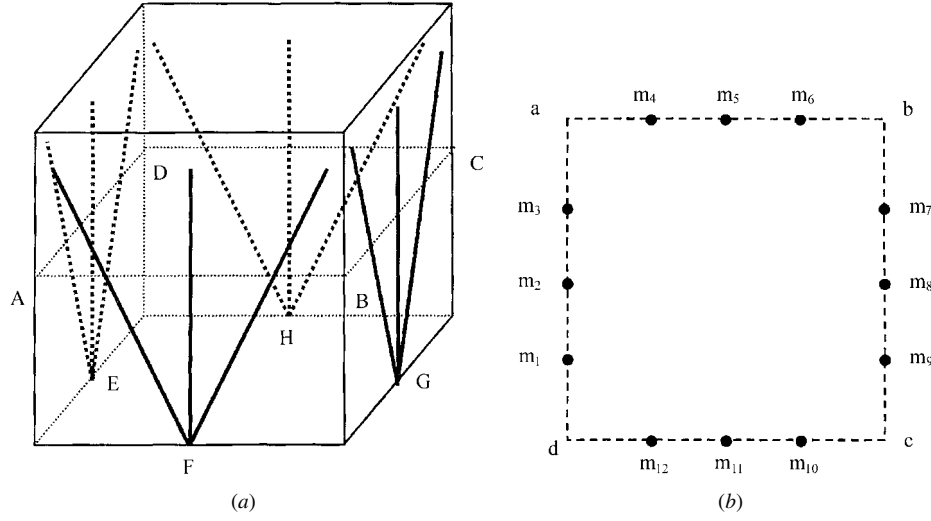


**Figure 1.** The structure of a head frame with V-shaped localization rods (a) (viewed from in front of a patient) and the distribution of localization markers in a transverse image (b) when the image is scanned while parallel to the frame base. The square  $ABCD$  is the scanning position of this image and corresponds to the square  $abcd$  in the image. Symbols  $m_1, m_2, \dots, m_{11}$  and  $m_{12}$  are markers.

following equation to represent this coordinate transformation:

$$\begin{pmatrix} X \\ Y \\ Z \end{pmatrix} = \begin{pmatrix} x - x_0 \\ y - y_0 \\ z \end{pmatrix} / k \quad (1)$$

where  $(x, y)$  are the coordinates of a point in the ICS and  $(X, Y, Z)$  are the corresponding coordinates of the point in the FCS;  $z$  is equal to  $m_1m_3, m_4m_6, m_7m_9$  or  $m_{10}m_{12}$ ;  $(x_0, y_0)$  are the coordinates of the centre of the square  $abcd$  in the ICS; and  $k$  is the image magnification factor, which is equal to the ratio of  $ab$  to  $AB$ ,  $bc$  to  $BC$ ,  $cd$  to  $CD$  and  $da$  to  $DA$ .

However, when transverse images are scanned obliquely, we do not observe these characteristics. Lines drawn through three markers of each localization plane result in a parallelogram (figure 2). The coordinate transformation between the ICS and the FCS includes not only translations but also rotations. In this case, the procedure for determining the coordinate transformation matrix can be divided into three steps.

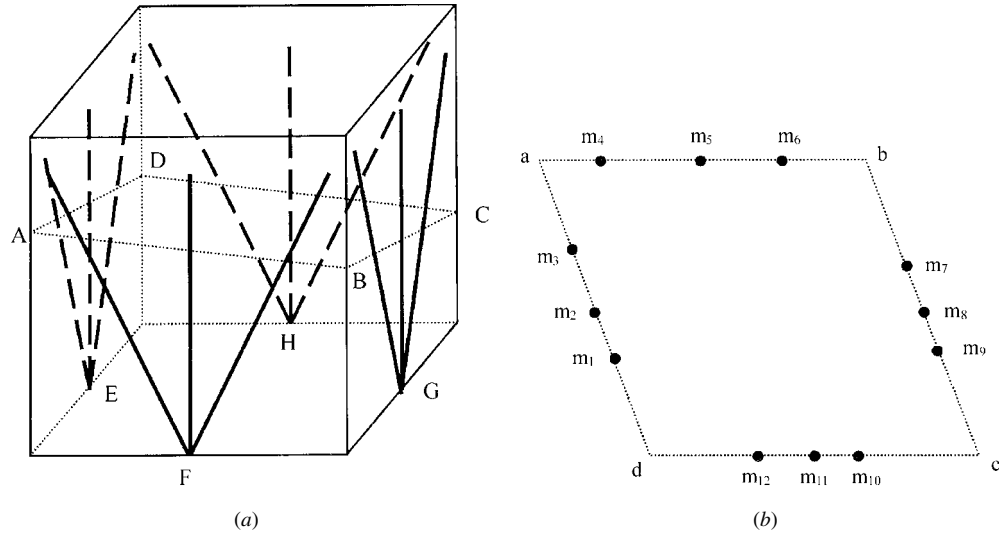
**2.1.1. Step 1: Calculate the oblique angles and the magnification factor.** The obliqueness of one transverse image relative to the frame base can be quantified by two angles. One angle, designated  $\alpha$ , is between line  $BA$  (or  $CD$ ) and the frame base. The other angle, designated  $\beta$ , is between line  $CB$  (or  $DA$ ) and the frame base.

Figure 3 shows the right localization plane of the head frame. On the basis of the design of the head frame

$$\angle M_1EM_2 = \angle M_2EM_3 = v \quad (2a)$$

$$\angle M_2M_1E = \pi/2 - v + \beta \quad (2b)$$

$$\angle M_2M_3E = \pi/2 - v - \beta. \quad (2c)$$



**Figure 2.** The structure of a head frame with V-shaped localization rods (a) and the distribution of localization markers in a transverse image (b) when this image is scanned obliquely. The parallelogram  $ABCD$  is the scanning position of this image and corresponds to the parallelogram  $abcd$  in the image. Symbols  $m_1, m_2, \dots, m_{11}$  and  $m_{12}$  are markers.

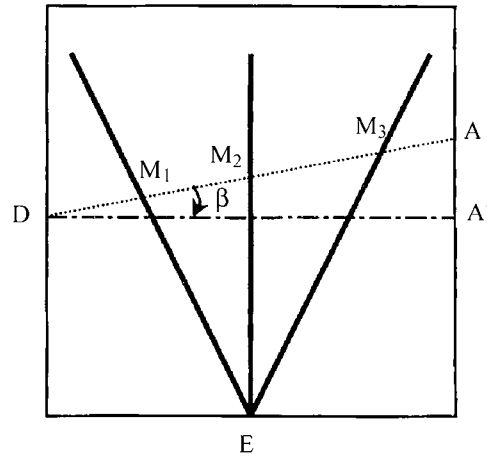


**Figure 3.** The right localization plane of the head frame. Symbols  $M_1, M_2$  and  $M_3$  are the intersection points of the scanned transverse plane and the right localization plane and correspond to markers  $m_1, m_2$  and  $m_3$  (shown in figure 2) respectively.

By using the law of sines, we determine that

$$\frac{M_2 E}{\sin(\pi/2 - v + \beta)} = \frac{M_1 M_2}{\sin(v)} \quad (3a)$$

$$\frac{M_2 E}{\sin(\pi/2 - v - \beta)} = \frac{M_2 M_3}{\sin(v)}. \quad (3b)$$

By dividing equation (3a) by equation (3b) we obtain the equation for the angle  $\beta$ , i.e.

$$\beta = \tan^{-1} \left( \frac{2(1 - M_1 M_2 / M_2 M_3)}{1 + M_1 M_2 / M_2 M_3} \right). \quad (4)$$

Because  $M_1M_2/M_2M_3 = m_1m_2/m_2m_3$ , equation (4) is transformed into

$$\beta = \tan^{-1} \left( \frac{2(1 - m_1m_2/m_2m_3)}{1 + m_1m_2/m_2m_3} \right). \quad (5a)$$

Similarly, by using all the markers in the other three localization planes, we obtain another equation for the angle  $\beta$  and two equations for the angle  $\alpha$ , i.e.

$$\beta = \tan^{-1} \left( \frac{2(1 - m_8m_9/m_7m_8)}{1 + m_8m_9/m_7m_8} \right) \quad (5b)$$

$$\alpha = \tan^{-1} \left( \frac{2(1 - m_5m_6/m_4m_5)}{1 + m_5m_6/m_4m_5} \right) \quad (5c)$$

$$\alpha = \tan^{-1} \left( \frac{2(1 - m_{10}m_{11}/m_{11}m_{12})}{1 + m_{10}m_{11}/m_{11}m_{12}} \right). \quad (5d)$$

Just as  $\beta$  may be determined by equation (5a) or (5b),  $\alpha$  may be determined by equation (5c) or (5d), we may use both equations and average the results. In case we encounter difficulty in identifying the image points, we can use one of the two equations.

The physical lengths of all four sides of the parallelogram  $ABCD$  are represented by

$$AB = CD = S/\cos \alpha, \quad BC = DA = S/\cos \beta \quad (6)$$

where  $S$  is the distance between each of two opposite localization planes.

Because the image magnification factor is defined as

$$k = ab/AB = bc/BC = cd/CD = da/DA \quad (7)$$

we substitute equation (6) into equation (7) and obtain the equation for calculating the image magnification factor:

$$\begin{aligned} k &= ab \cos \alpha / S = bc \cos \beta / S \\ &= cd \cos \alpha / S = da \cos \beta / S. \end{aligned} \quad (8)$$

Again, we can use any or all of the equations (by averaging the results) to calculate the magnification factor.

**2.1.2. Step 2: Determine the coordinates of four markers.** We should use the coordinates of the second, fifth, eighth and eleventh markers to determine the coordinate transformation matrix between the ICS and the FCS as there are no simple ways to use other markers for such a purpose. The coordinates of these four markers in the ICS can be detected manually or automatically. On the basis of the design of the head frame, the  $X, Y$  coordinates of the four markers in the FCS are given as

$$\begin{aligned} X_2 = S/2 \quad Y_2 = 0 \quad X_5 = 0 \quad Y_5 = S/2 \quad X_8 = -S/2 \quad Y_8 = 0 \\ X_{11} = 0 \quad Y_{11} = -S/2. \end{aligned} \quad (9)$$

The  $Z$  coordinates of the four markers in the FCS are equal to the lengths of lines  $M_2E$ ,  $M_5F$ ,  $M_8G$  and  $M_{11}H$  respectively. By using equations (3a) and (3b) we obtain

$$\begin{aligned} M_2E &= M_1M_2 \sin(\pi/2 - v + \beta)/\sin(v) \\ &= M_2M_3 \sin(\pi/2 - v - \beta)/\sin(v). \end{aligned} \quad (10)$$

Substituting  $Z_2$  for  $M_2E$ ,  $m_1m_2/k$  for  $M_1M_2$  and  $m_2m_3/k$  for  $M_2M_3$ , we obtain

$$\begin{aligned} Z_2 &= 2.236m_1m_2 \sin(\pi/2 - v + \beta)/k \\ &= 2.236m_2m_3 \sin(\pi/2 - v - \beta)/k. \end{aligned} \quad (11a)$$

Similarly, the  $Z$  coordinates of the fifth, eighth and eleventh markers in the FCS can be represented by

$$\begin{aligned} Z_5 &= 2.236m_4m_5 \sin(\pi/2 - v - \alpha)/k \\ &= 2.236m_5m_6 \sin(\pi/2 - v + \alpha)/k \end{aligned} \quad (11b)$$

$$\begin{aligned} Z_8 &= 2.236m_7m_8 \sin(\pi/2 - v - \beta)/k \\ &= 2.236m_8m_9 \sin(\pi/2 - v + \beta)/k \end{aligned} \quad (11c)$$

$$\begin{aligned} Z_{11} &= 2.236m_{10}m_{11} \sin(\pi/2 - v + \alpha)/k \\ &= 2.236m_{11}m_{12} \sin(\pi/2 - v - \alpha)/k. \end{aligned} \quad (11d)$$

*2.1.3. Step 3: Determine the coordinate transformation.* According to the principle of rigid body transformation, the coordinate transformation between the ICS and the FCS can be represented by

$$X = a_1x + b_1y + c_1 \quad Y = a_2x + b_2y + c_2 \quad Z = a_3x + b_3y + c_3. \quad (12)$$

We can rewrite equation (12) in a matrix form,

$$\begin{pmatrix} X \\ Y \\ Z \end{pmatrix} = \begin{pmatrix} a_1 & b_1 & c_1 \\ a_2 & b_2 & c_2 \\ a_3 & b_3 & c_3 \end{pmatrix} \begin{pmatrix} x \\ y \\ 1 \end{pmatrix} = \text{MIF} \begin{pmatrix} x \\ y \\ 1 \end{pmatrix} \quad (13)$$

where  $a_i$ ,  $b_i$  and  $c_i$  are constants to be determined ( $i = 1, 2$ , and  $3$ ). The abbreviation MIF is the coordinate transformation matrix from the ICS to the FCS.

Substituting the coordinates of the second, fifth, eighth, and eleventh markers into equation (12), we obtain three groups of linear equations. Because each group has four equations and three variables ( $a_i$ ,  $b_i$  and  $c_i$ ), the groups are over-determined. This problem can be solved by the linear least square method (Stanek 1996). The transformation matrix in equation (13) is valid only for the image slice under consideration and must be recalculated for all other image slices.

### 3. Discussion

As shown in equations (5), (6) and (9), we can calculate the oblique angles and the image magnification factor for each slice. In clinical practice, all slices imaged are usually parallel to each other, in the same spatial resolution. Therefore, the oblique angles and the image magnification factor should be the same for all slices. Disagreement in the values of these three parameters from different slices suggests potential errors in detecting the positions of the markers on some slices. The possibility of error in detecting the positions of the markers is the same for all slices, and the distance between any two of the three markers of a localization plane increases when the slice to be scanned is farther away from the frame base. Therefore, the accuracy of calculating these three parameters also increases. This fact suggests that it is better to use the values of the three parameters that are determined for those slices farther away from the frame base than those that are determined for those slices near the frame base.

As shown in equation (13), there are nine unknown variables, but these variables are not all independent. In fact, they can be represented as trigonometric functions of three translation variables and three rotation variables. Because there is no simple method for solving groups of trigonometric equations, we choose to solve groups of linear equations instead at a cost of three additional variables.

#### 4. Conclusion

Our proposed algorithm can be used to determine the coordinate transformation for stereotactic localization in CT or MR transverse imaging. The algorithm takes into consideration the fact that the positioning of a patient may result in transverse images that are not parallel to the frame base. Thus there is no need to adjust the position of the localization frame manually before CT or MR imaging is performed. Therefore, this algorithm is robust in principle and is useful for improving the accuracy and efficiency of localization.

#### Acknowledgments

This investigation was supported in part by a cooperative grant from CREAT Electronic Technology Inc.; by a Whitaker Foundation Biomedical Engineering grant; by grant R29 CA65606 and Cancer Center Support (CORE) grant P30 CA 21765 from the National Cancer Institute; and by the American Lebanese Syrian Associated Charities (ALSAC). The authors thank Chen-Shou Chui, PhD, for a critical reading of the manuscript.

#### References

- Brown R A, Roberts T S and Osborn A G 1980 Stereotaxic frame and computer software for CT-directed neurosurgical localization *Invest. Radiol.* **15** 308–12
- Grunert P and Maurer J 1995 Target point calculation in the computerized tomography. Comparison of different stereotactic methods *Neurosurg. Rev.* **18** 15–24
- Hartmann G H, Bauer-Kirpes B, Serago C F and Lorenz W J 1994 Precision and accuracy of stereotactic convergent beam irradiations from a linear accelerator *Int. J. Radiat. Oncol. Biol. Phys.* **28** 481–92
- Hartmann G H, Schlegel W, Sturm V, Kober B, Pastyr O and Lorenz W J 1985 Cerebral radiation surgery using moving field irradiation at a linear accelerator facility *Int. J. Radiat. Oncol. Biol. Phys.* **11** 1185–92
- Leksell L 1983 Stereotactic radiosurgery *J. Neurol. Neurosurg. Psych.* **46** 797–803
- Lutz W, Winston K R and Maleki N 1988 A system for stereotactic radiosurgery with a linear accelerator *Int. J. Radiat. Oncol. Biol. Phys.* **14** 373–81
- Saw C B, Ayyangar K and Suntharalingam N 1987 Coordinate transformations and calculation of the angular and depth parameters for a stereotactic system *Med. Phys.* **14** 1042–4
- Serago C F, Lewin A A, Houdek P V, Gonzalez-Arias S, Hartmann G H, Abitbol A A and Schwade J G 1991 Stereotactic target point verification of an X-ray and CT localizer *Int. J. Radiat. Oncol. Biol. Phys.* **20** 517–23
- Siddon R L and Barth N H 1987 Stereotactic localization of intracranial targets *Int. J. Radiat. Oncol. Biol. Phys.* **13** 1241–6
- Stanek G 1996 Scientific computing *Standard Mathematical Tables and Formulae* 30th edn, ed D Zwillinger, K H Rosen and S Z Krantz (Boca Raton, FL: CRC) pp 681–2
- Yeung D, Palta J, Fontanesi J and Kun L 1994 Systematic analysis of errors in target localization and treatment delivery in stereotactic radiosurgery (SRS) *Int. J. Radiat. Oncol. Biol. Phys.* **28** 493–8